ORIGINAL RESEARCH

Aging is Associated With an Earlier Arrival of Reflected Waves Without a Distal Shift in Reflection Sites

Timothy S. Phan, BSBME, BSECE, MSEE; John K.-J. Li, PhD; Patrick Segers, PhD; Maheswara Reddy-Koppula, MD; Scott R. Akers, MD, PhD; Samuel T. Kuna, MD; Thorarinn Gislason, MD, PhD; Allan I. Pack, MBChB, PhD; Julio A. Chirinos, MD, PhD

***Background*—**Despite pronounced increases in central pulse wave velocity (PWV) with aging, reflected wave transit time (RWTT), traditionally defined as the timing of the inflection point (T_{INF}) in the central pressure waveform, does not appreciably decrease, leading to the controversial proposition of a "distal-shift" of reflection sites. T_{INF}, however, is exceptionally prone to measurement error and is also affected by ejection pattern and not only by wave reflection. We assessed whether RWTT, assessed by advanced pressure-flow analysis, demonstrates the expected decline with aging.

***Methods and Results*—**We studied a sample of unselected adults without cardiovascular disease (n=48; median age 48 years) and a clinical population of older adults with suspected/established cardiovascular disease (n=164; 61 years). We measured central pressure and flow with carotid tonometry and phase-contrast MRI, respectively. We assessed RWTT using wave-separation analysis ($RWTT_{WSA}$) and partially distributed tube-load (TL) modeling ($RWTT_{TL}$). Consistent with previous reports, T_{INF} did not appreciably decrease with age despite pronounced increases in PWV in both populations. However, aging was associated with pronounced decreases in $RWTT_{WSA}$ (general population −15.0 ms/decade, $P<0.001$; clinical population −9.07 ms/decade, $P=0.003$) and $RWTT_{TL}$ (general −15.8 ms/decade, $P<0.001$; clinical −11.8 ms/decade, $P<0.001$). There was no evidence of an increased effective reflecting distance by either method. T_{INF} was shown to reliably represent RWTT only under highly unrealistic assumptions about input impedance.

***Conclusions*—**RWTT declines with age in parallel with increased PWV, with earlier effects of wave reflections and without a distal shift in reflecting sites. These findings have important implications for our understanding of the role of wave reflections with aging.
(*J Am Heart Assoc*. 2016;5:e003733 doi: 10.1161/JAHA.116.003733)

Key Words: aging • effective reflective distance • pulse wave velocity • reflection timing • wave reflections

Pulsatile arterial hemodynamics is highly relevant for cardiovascular disease associated with aging and various disease states.[1] Several studies have demonstrated that both aortic pulse wave velocity (PWV) and measures of wave reflections are independently predictive of cardiovascular disease.[2-6] Pulse waves generated by the heart travel forward in the arteries at a finite PWV and undergo partial reflections at sites of impedance mismatch (such as points of branching or changes in wall diameter or material properties along the arterial tree). Innumerable reflections effectively merge into a discrete reflected wave, as seen from the aortic root, increasing aortic pulse pressure and left ventricular pulsatile afterload.

With increasing PWV, the speed of forward and backward wave travel increases, which is logically expected to result in an earlier arrival of wave reflections. However, the increased large artery PWV with aging has been reported to be associated with unremarkable changes in the time of the inflection point (T_{INF}) of the central pressure waveform in mid- to late adulthood, traditionally defined as reflection timing.[3,7,8] If T_{INF} is interpreted as a surrogate of reflected wave transit time (RWTT), this combination would appear to represent an increase in effective reflective distance. Along with the observation that there is little increase in medium-sized (muscular artery) PWV with aging in the setting of

From the Rutgers University, Piscataway, NJ (T.S.P., J.K.-J.L.); University of Pennsylvania Perelman School of Medicine, Philadelphia, PA (T.S.P., M.R.-K., S.R.A., S.T.K., A.I.P., J.A.C.); Ghent University, Ghent, Belgium (P.S., J.A.C.); Corporal Michael J. Crescenz VAMC, Philadelphia, PA (S.R.A., S.T.K., J.A.C.); Department of Respiratory Medicine and Sleep, Landspitali—The National University Hospital of Iceland, Reykjavik, Iceland (T.G.); Faculty of Medicine, University of Iceland, Reykjavik, Iceland (T.G.).

Accompanying Datas S1, S2 and Figures S1 through S6 are available at http://jaha.ahajournals.org/content/5/9/e003733/DC1/embed/inline-supplementary-material-1.pdf

This article was handled by Christopher M. Kramer, MD, as a guest editor. The editors had no role in the evaluation of this manuscript or in the decision about its acceptance.

Correspondence to: Timothy S. Phan, BSBME, BSECE, 3400 Civic Center Blvd, PCAM-South Tower 11th Fl, Philadelphia, PA 19104. E-mail: timphan@med.upenn.edu

Received April 15, 2016; accepted July 11, 2016.

increased large artery PWV, the lack of change in T_{INF} with aging has motivated the controversial[9] proposition that aging is associated with impedance matching of central and peripheral arteries and a distal shift of reflection sites.[10-12] This proposition has been advanced as a key mechanism for aging-related microvascular disease. However, it challenges established principles of pulse wave transmission and reflection[8,13-15] and is based on the untenable assumption that "PWV matching" is equivalent to impedance matching.[16] Furthermore, the inaccuracy of relying on T_{INF} (a high-frequency pressure-only characteristic point exceptionally prone to measurement error) as a surrogate of RWTT has been demonstrated in humans[17] and modeling studies.[18] T_{INF} is also highly dependent on factors other than arterial wave reflection timing, including the pattern of LV contraction.[19,20] Therefore, it remains unclear whether aging is indeed associated with an earlier arrival of wave reflections, an issue that has important implications for our understanding of the role of wave reflections and microvascular disease with aging.

The aim of the present study was to assess whether aging is indeed associated with a distal shift in reflecting sites (as suggested by previous studies that utilized T_{INF}), using appropriate pressure-flow analyses. We also aimed to critically assess underlying assumptions and limitations of various techniques to compute RWTT and their implications for the assessment of aging-related changes in RWTT and effective reflective distance.

Methods

Study Population

We performed 2 substudies.

1. *Substudy in adult participants from an unselected population.* We enrolled a sample of adult volunteers (n=48, median age 49 years) at the University of Pennsylvania and the University of Iceland as part of the control population for the Penn-Iceland Sleep Apnea Study. Participants were adults without overt cardiovascular disease who were on stable medications (no changes in the 2 months prior to enrollment). We excluded subjects with a history of obstructive sleep apnea or any sleep disorder, a body mass index >40 kg/m^2, a positive urine toxicology screen, routine consumption of >2 alcoholic beverages per day, current/recent illicit drug use, excessive caffeine use (>10 caffeinated beverages per day), active infection, malignancy, chronic inflammatory disorders, atrial fibrillation, or inability to undergo a cardiac MRI. Women with a positive pregnancy test or who were receiving hormone replacement therapy were excluded from the study.
2. *Substudy in an older clinical population.* Given that the impact of pulsatile hemodynamics and the proposition of a distal shift of reflecting sites with aging are particularly relevant for older patients with cardiovascular risk factors or established cardiovascular disease, we also studied a population of older adults (n=164, median age 61 years) with established or suspected cardiovascular disease referred for a cardiac MRI examination at the Corporal Michael J. Crescenz Veterans Affairs Medical Center (VAMC) or the Hospital of the University of Pennsylvania.

The institutional review boards of the VAMC, University of Pennsylvania, and University of Iceland approved the parent studies, and all subjects provided written informed consent.

MRI Examinations

We measured ascending aortic flow with phase-contrast MRI, using 1.5-T Avanto or Espree systems (Siemens Medical Solutions). A phase-contrast gradient-echo pulse sequence with through-plane velocity encoding was applied during free breathing using retrospective gating, in a plane perpendicular to the long axis of the proximal ascending aorta. Maximal velocity encoding was set at 150 cm/s, adjusted as needed to avoid aliased velocity measurements. Other typical parameters were slice thickness 6 mm, matrix 192×192, and repetition time $\approx$10 milliseconds. Images were analyzed using the freely available software Segment.[21] Flow-time integrals were scaled to stroke volume measured with cine steady-state free precession (SSFP) images of the left ventricle (short-axis stack) in order to minimize errors introduced by phase-offset and eddy currents. Carotid-femoral PWV was measured with a SphygmoCor EM3 device (AtCor Medical, Sydney, Australia), with sequential tonometry recordings of the carotid and femoral pulse, using the QRS complex as a fiducial time point.

Reflected Wave Transit Time

We utilized 3 methods to compute RWTT.

Method 1. T_{INF} was calculated as the time from the foot of the carotid pressure waveform to the inflection point (Figure 1A) as identified by the SphygmoCor platform (C_T1R variable).

Method 2. Wave separation analysis (WSA) was performed on time-aligned pressure and flow signals using standard methods.[22] Briefly, arterial input impedance (Z_{in}) was derived using Fourier analysis as the ratio of pressure to flow harmonics in the frequency domain. Aortic characteristic impedance (Z_c) was estimated by averaging the modulus of Z_{in} for harmonics 3 to 15. Only harmonics with flow magnitudes >5% of the fundamental harmonic flow

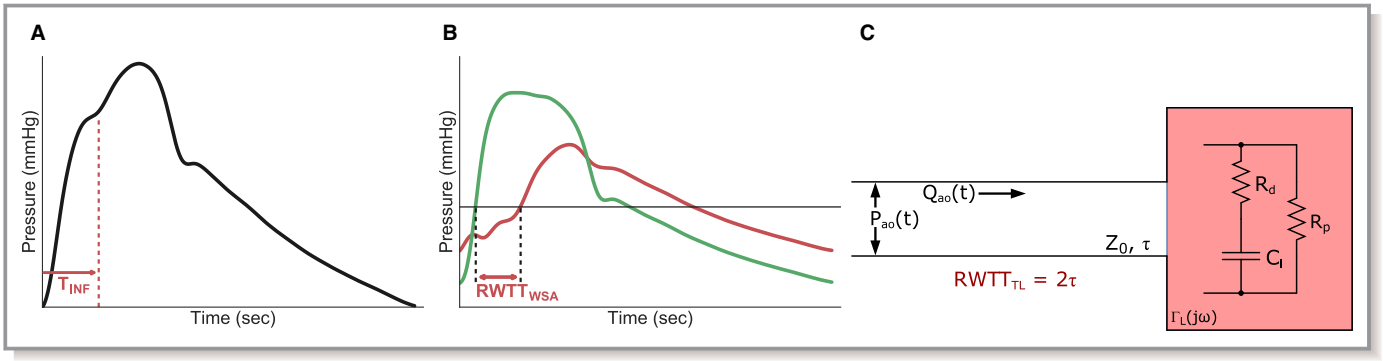

Figure 1. Assessment of T_{INF} (A) and of RWTT via WSA (B) and TL modeling (C). In WSA, forward and backward waves are computed from pressure-flow data, and the time delay between the point at which backward (red) and forward (green) pressure waves start adding to mean pressure (zero crossing) is considered as the RWTT. TL modeling utilizes the entire pressure and flow information to assess the 1-way wave transit time (τ) to the reflection site (which is complex and frequency dependent, as indicated in the shaded red region); RWTT was obtained as twice the value of τ.

magnitude were included in the averaging process to minimize the effects of noise.[23] Forward (P_f) and backward (P_b) pressure waves were obtained from the relations $P_f=(P+QZ_c)/2$ and $P_b=(P-QZ_c)/2$. Time-varying P_f and P_b waveforms were obtained through inverse Fourier transformation. Because the "foot" of P_f and P_b is generally not well defined and particularly susceptible to sources of high-frequency noise (eg, measurement, Z_c estimation method), $RWTT_{WSA}$ was calculated as the time delay between the zero crossings of P_f and P_b as previously described[17] (Figure 1B), due to better definition of the landmarks. Despite improved definition of zero crossings over the "foot" of P_b and P_f, a small subset of cases had poorly defined zero crossings (Figure S1).

Method 3 (TL modeling). The arterial system was modeled as a finite PWV system represented by a lossless tube terminating in a complex frequency-dependent load (Figure 1C).[24,25] Tube-based models with complex loads have been previously validated and applied to various animal species[25–28] and humans[29,30] for the purpose of studying arterial wave reflections. The TL model used here is fully characterized by tube characteristic impedance (Z_0), peripheral resistance (R_p), load compliance (C_I), and 1-way wave transmission time to the effective reflection site (τ). R_p was calculated as the ratio of mean pressure to mean flow. With measured aortic flow as input to the model, an optimal set of parameters (Z_0, C_I, τ) was obtained after minimizing the normalized root mean square error (NRMSE) of predicted and measured pressure; a unique set of parameters can be identified if τ multiplied by a measurement of PWV is within the dimensions of the body.[31] NRMSE was calculated as the square root of the mean squared error normalized by mean arterial pressure. $RWTT_{TL}$ was computed as twice the value of τ, to account for roundtrip travel, allowing for direct comparisons with T_{INF} and $RWTT_{WSA}$.

Effective Reflection Distance

Combining RWTT with measured carotid-femoral PWV allows for calculation of an effective reflection distance (ERD). If wave reflections, as seen from the proximal aorta, were to be summarized and abstracted by a *theoretical* single discrete reflection site from which all reflections effectively originate, ERD represents the distance to this site. ERD was calculated as $0.5\times RWTT\times PWV$.

Assumed Input Impedance Spectra of T_{INF} and TL Modeling

The computation of an ERD from T_{INF} and PWV relies on the assumption that a uniform tube, terminated in a peripheral resistance (ie, a real reflection coefficient), represents a suitable approximation of the arterial system.[32–35] This model's input impedance ($Z_{in,INF}$) can be fully specified by 3 parameters (see Data S1): aortic Z_c, 1-way tube transit time ($0.5\times T_{INF}$), and R_p. We used this model, as well as TL modeling (Method 3) to generate input impedance spectra for each decade of age in order to assess the correspondence of each model with the known age-related changes to input impedance patterns.

Statistical Analysis

Continuous variables are reported as mean±standard deviation or median and interquartile range (IQR), as appropriate. Proportions are expressed as percentages. Changes with age are presented as point estimates and 95% confidence intervals (CIs) for each decade of life. We used linear regression analysis to compute the mean change per decade of age in RWTT and ERD, as estimated by each of the 3 methods described above. Statistical significance was defined as a 2-tailed $\alpha<0.05$. Statistical analyses were performed using SPSS (SPSS Inc, Chicago, IL).

Results

Tables 1 and 2 list the clinical and hemodynamic characteristics, respectively, of study subjects in the general sample and the clinical sample.

Changes in PWV, RWTT, and ERD With Aging

Figure 2 demonstrates trends of PWV as well as RWTT and ERD computed by the 3 methods for the general sample (Figure 2A) and the clinical sample (Figure 2B). We observed the well-known increase in PWV across decades of age (Figure 2A and 2B, top row), with a mean per-decade increase of 0.80 m/s (95% CI=0.48-1.12; $P<0.001$) in the general population sample and 1.34 m/s (95% CI=0.85-1.82; $P<0.001$) in the clinical sample. Similarly, consistent with previous reports, T_{INF} exhibited minimal changes across decades of age in either the general sample (Figure 2A; ß=−5.41 ms per decade; 95% CI=−1.07 to −0.15; $P=0.044$) or the clinical sample (Figure 2B; ß=−0.34 ms per decade; 95% CI=−0.380 to −0.312; $P=0.85$). T_{INF} remained within a very narrow range in both samples after the fourth decade of life (Figure 2A and 2B, middle panels). For instance, in the clinical sample, it decreased from a mean of 152 milliseconds for subjects <40 years old to 145 milliseconds for subjects aged 70 to 79 years old, representing a 4.6% decrease in timing despite a 67.0% increase in carotid-femoral PWV. As a result, apparent ERD computed by the inflection point timing (ERD_{INF}) increased with age in both the general (ß=5.46 cm/decade; 95% CI=1.86-9.06; $P=0.004$) and clinical samples (ß=9.27 cm/decade; 95% CI=5.70-12.8; $P<0.001$; Figure 2A and 2B, bottom panels), consistent with previous reports that relied on T_{INF} as a surrogate for RWTT.

Results were, however, markedly different when methods derived from pressure-flow data were used to estimate reflection timing. WSA and TL modeling demonstrated pronounced and significant reductions in RWTT across decades of age (Figure 2A and 2B, middle panels). $RWTT_{WSA}$ decreased by −15.0 milliseconds per decade of age (95% CI=−2.142 to −8.7; $P<0.001$) in the general sample and −9.07 milliseconds (95% CI=−14.9 to −3.2; $P=0.003$) in the clinical sample, with the latter sample demonstrating consistently lower times (ie, earlier wave reflections) across the age spectrum than the general population sample. Similarly, TL modeling indicated that RWTT decreased by −15.8 milliseconds per decade of age (95% CI=−2.11 to −1.04; $P<0.001$) in the general sample and by −11.8 milliseconds (95% CI=−15.3 to −8.2; $P<0.001$) in the clinical sample, with the clinical sample demonstrating consistently lower times across the age spectrum than the general population sample. The overall decrease in RWTT with aging across the life span was pronounced. In the clinical sample, for instance, $RWTT_{TL}$ decreased by 62.7% from <40 years old to 70 to 79 years.

Given that the reduction in $RWTT_{WSA}$ was concordant with the increase in PWV, ERD computed by this method was found to not significantly increase with age in either the general sample (ß=0.78 cm/decade; 95% CI=−2.4 to 4.0; $P=0.63$) or the clinical sample (ß=3.0 cm/decade; 95% CI=−1.47 to 7.44; $P=0.19$), with values consistently in the range of

Table 1. Clinical Characteristics of Subjects Enrolled in Both Substudies

	General Sample (n=48)	Clinical Sample (n=164)
Age, y	49 (43, 54)	61 (54, 66)
Male	79 (38)	152 (93)
BMI, kg/m^2	26.8 (24.9, 29.5)	29.8 (26.3, 33.9)
Height, cm	175 (169, 182)	175 (170, 183)
Hypertension	11 (23)	134 (82)
Current smoking	10 (21)	53 (32)
Diabetes mellitus	4 (8)	76 (46)
CAD	0 (0)	67 (41)
HF	0 (0)	68 (41)
ACE-I	4 (8)	79 (48)
ARB	3 (6)	21 (13)
β-Blocker	1 (2)	93 (57)
Long-acting nitrate	0 (0)	21 (13)
CCB	1 (2)	41 (25)

Values reported as median (IQR) or proportions expressed in percentage. ACE-I indicates angiotensin-converting enzyme inhibitor; ARB, angiotensin receptor blocker; BMI, body mass index; CAD, coronary artery disease; CCB, calcium channel blocker; HF, heart failure.

Table 2. Hemodynamic Characteristics of Study Subjects

	General Sample (n=48)	Clinical Sample (n=164)
MAP, mm Hg	88 (84, 97)	103 (94, 113)
Central SBP, mm Hg	114 (109, 122)	135 (123, 150)
Central PP, mm Hg	46 (41, 51)	53 (45, 68)
Heart rate, BPM	66 (62, 71)	62 (55, 71)
Cardiac output, L/min	6.6 (5.3, 7.5)	5.01 (3.7, 6.4)
SVR, dynes·s/cm^5	1162 (955, 1346)	1632 (1315, 2170)
Z_c, dynes·s/cm^5	81.0 (66.6, 93.1)	103 (80, 140)
Reflection coefficient magnitude, $\|\Gamma_1\|$	0.48 (0.41, 0.53)	0.50 (0.41, 0.56)
Reflection coefficient phase θ_1, deg	−60.3 (−71.2, −49.5)	−45.4 (−56.9, −35.6)
PWV, m/s	7.0 (6.1, 7.8)	9.6 (7.8, 11.4)

Values reported as median (IQR). BPM indicates beats per minute; MAP, mean arterial pressure; PP, pulse pressure; PWV, pulse wave velocity; SBP, systolic blood pressure; SVR, systemic vascular resistance; Z_c, aortic characteristic impedance.

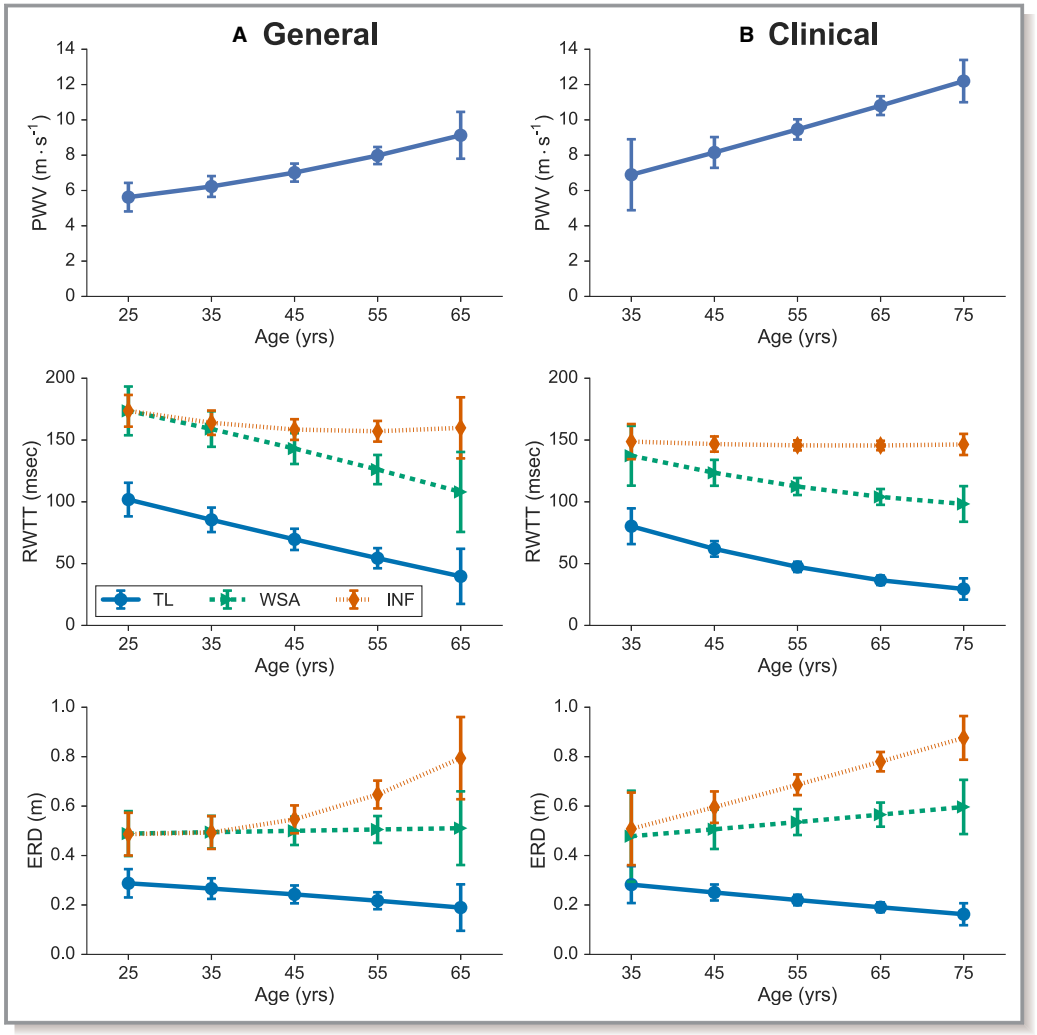

Figure 2. Change in carotid-femoral PWV with aging (top), RWTT (middle), and ERD (bottom) in the general population sample (A, left panels) and the clinical sample (B, right panels).

~50 cm. Given the pronounced reduction of $RWTT_{TL}$ with age (Figures 2 and 3), aging was associated with a decrease in ERD_{TL} in both the general population sample (ß=−2.37 cm per decade; 95% CI=−4.63 to −0.17; *P*=0.04) and the clinical sample (ß=−2.96 cm per year decade 95% CI=−4.77 to −1.16; *P*=0.001).

Interpretations of Reflection Timing and ERD

Figure 3 summarizes the competing interpretations of wave reflection timing and effective reflection distance for the general population and the clinical samples. Each point corresponds to the mean change in the variable per decade of age, with error bars denoting 95% CIs. In both populations, PWV increases with age, particularly in the clinical sample. The green region demonstrates analyses based on pressure only (T_{INF}), which demonstrates a very small decrease in T_{INF} with age in the general sample and a nonsignificant change in the clinical sample. When interpreted in the context of the markedly increased PWV, the apparent ERD by this method increases, suggesting a distal shift of reflecting sites, consistent with previous reports.[7,10-12] These results, however, are not supported by analyses that use pressure and flow data. The red-shaded region shows results from WSA, demonstrating significant decreases in $RWTT_{WSA}$ concordant with the increase in PWV in both samples, without significant changes to ERD_{WSA}, which is inconsistent with a distal shift of reflection sites with age. Furthermore, TL modeling (blue-shaded region) demonstrates pronounced decreases in $RWTT_{TL}$, with a *decreased* ERD_{TL} with age (ie, effective reflection sites move closer, rather than further away from to the heart with aging).

Assumptions of T_{INF} as a Surrogate of RWTT for Assessments of ERD

Input impedance patterns per decade of age implied by use of T_{INF} and PWV for the calculation of ERD_{INF} are shown in Figure S2A for the clinical sample and Figure S3A for the

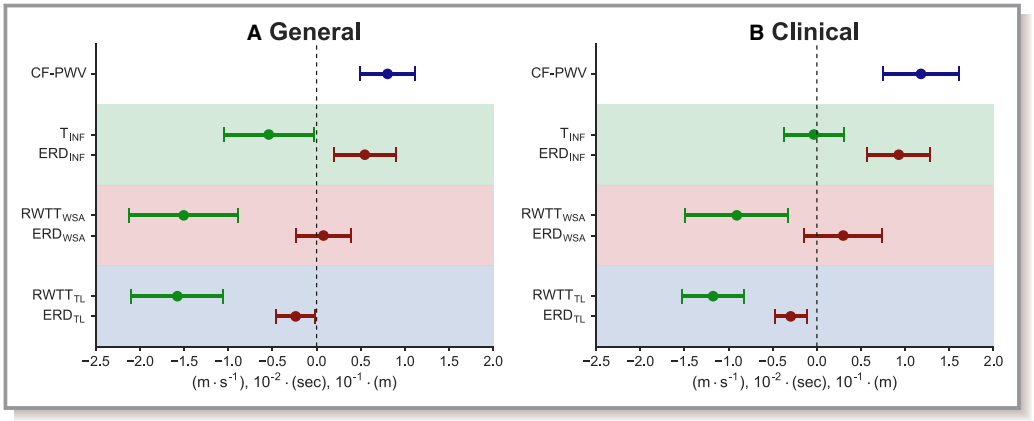

Figure 3. Estimated change in carotid-femoral PWV (blue bars), RWTT (green bars), and ERD (red bars) per decade of life, assessed by different methods, in the general population sample (A, left panels) and the clinical sample (B, right panels). The green-shaded area represents assessments from the inflection point timing (T_{INF}). The red-shaded area represents assessments from the use of WSA. The blue area demonstrates estimates from use of TL modeling.

general sample. The figures demonstrate markedly unrealistic impedance patterns, based on known input impedance patterns reported in the literature, with apparently high reflections occurring in the higher frequencies. In sharp contrast, input impedance patterns implied by the TL model (Figures S2B and S3B) in the same populations are highly consistent with the well-known human input impedance patterns and their changes with aging, including a shift to higher frequencies of the magnitude minima and the zero crossover of the phase angle of input impedance. Two examples for comparison of the time-domain pressure-flow relationships implied by the models are shown in rows I and II of Figure 4. It is clear that use of T_{INF} as a surrogate for the arrival of reflection waves is highly inconsistent with the relationship between measured pressure and flow; predicted pressure waveforms are highly oscillatory and are nonphysiological. Because losses in the large arteries are small, similar results are obtained when the tube is viscoelastic.[36]

Discussion

In this study, we assessed whether aging is associated with an increased ERD (ie, a distal shift in reflection sites), as suggested by studies that used T_{INF} as a surrogate of RWTT. In line with these previous reports, we found that carotid-femoral PWV increases markedly with aging, without an appreciable decrease in T_{INF}, falsely suggesting an increase in ERD. However, given the important limitations of T_{INF} as a surrogate of RWTT, and in contrast with previous studies that suggested a distal shift of reflecting sites, we quantified RWTT based on pressure-flow analyses. We demonstrate that RWTT markedly declines with age as PWV increases, with an earlier arrival of wave reflections and without a distal shift in reflecting sites. In fact, consistent with physiologic insights, TL modeling (which accounts for phase shifts associated with wave reflections), suggests that the ERD actually decreases (ie, reflections effectively move closer to the heart) as PWV increases with age.[17,35] We further demonstrate that T_{INF} is a misleading surrogate of RWTT with aging and would be reliably related to the latter only under highly unrealistic assumptions about human aortic input impedance patterns. We therefore reconcile the apparent paradox introduced by misinterpretation of T_{INF} as a surrogate of RWTT, disproving the proposition of a distal shift in reflecting sites with aging. Our findings have important implications for our understanding of the role of wave reflections on changes in arterial pulsatile hemodynamics with aging and their role in target organ damage and microvascular disease.

As shown in previous studies,[3,7,10,12,17] we found that T_{INF} in the central pressure waveform demonstrates unremarkable changes with age. Our estimates of T_{INF} essentially reproduce the pattern reported by Mitchell et al,[7] in which T_{INF} is constrained within tight limits across the adult age spectrum despite the sharp increase in carotid-femoral PWV. This has been interpreted as a distal shift of reflection sites[10,12] under the assumption that T_{INF} represents RWTT. Given the proposed central role of this distal shift on microvascular damage, carefully assessing this issue with appropriate methods is of great importance. Our findings demonstrate that T_{INF} is a poor measure of RWTT. There are several reasons for this. First, this characteristic point is dependent on high frequencies, which are most susceptible to measurement noise. In addition, T_{INF} is highly dependent on factors other than arterial wave reflection timing, including the pattern of LV contraction.[19,20] This is consistent with recent data demonstrating that the augmentation index (which is

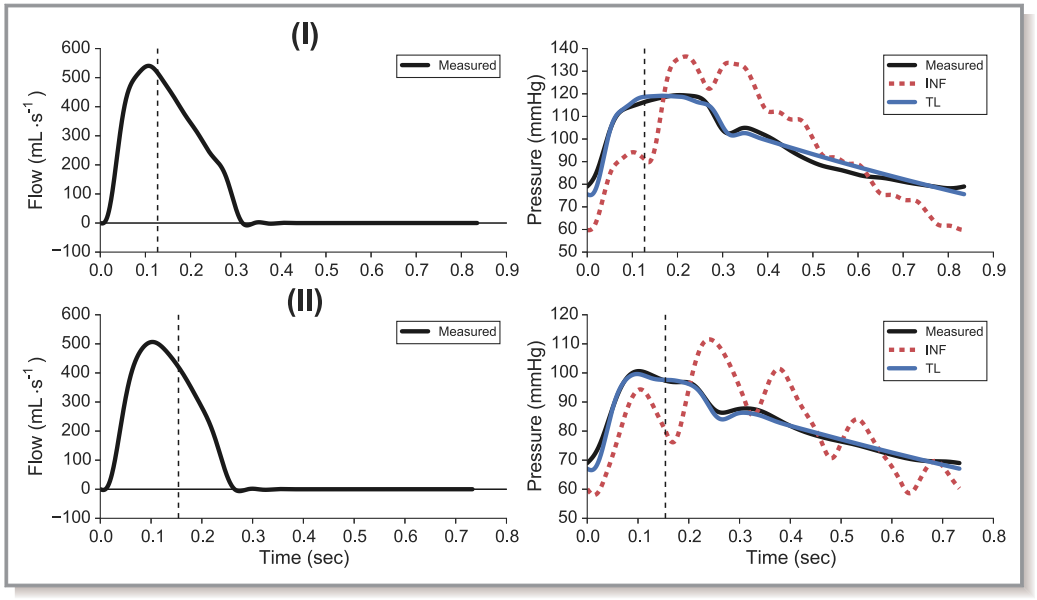

Figure 4. Model-predicted pressure waveforms when measured aortic flows are used as input into the underlying models assumed by the quarter-wavelength formula used with T_{INF} as reflection timing (INF) and TL modeling. The vertical dashed lines indicate T_{INF} as identified by the SphygmoCor system.

computed based on the pressure at the inflection point) is influenced by various factors other than wave reflections and is not a robust predictor of cardiovascular risk.[5,37]

The primary derivation of the inflection point as a surrogate for RWTT explicitly assumed an arterial system model as a uniform tube terminated with a pure resistance.[33] The profound limitations introduced by this assumption are often unrecognized. When implied input impedances from such a model are produced across the life span from measured parameters, its poor resemblance to the arterial system becomes readily apparent, with impedance patterns that show pronounced/unrealistic oscillations in both magnitude and phase spectra. These patterns are inconsistent with well-known patterns of human aortic input impedance,[33,38,39] characterized by modulus values settling around aortic Z_c as well as increasing frequency of the magnitude minimum and phase zero crossing with increasing age.[35,40,41] The assumption that T_{INF} can be used to infer ERD also implies a real reflection coefficient at the effective reflection site, which is inconsistent with the complex (and frequency-dependent) reflection coefficients that occur in vivo.[40,42,43] For instance, in the femoral arteries, reflection coefficients have frequency-dependent magnitudes, with the highest magnitudes in lower frequencies and magnitudes settling toward lower nonzero values in the higher frequencies.[40,44-46]

To avoid these important limitations, we used the TL model, which is terminated with a complex frequency-dependent load. We found that input impedance patterns derived from this model (using parameters obtained from both studied populations) display the well-known characteristics of human input impedance (Figures S2B and S3B), with a shift of the modulus minimum and phase zero crossing to increasing frequency with increasing age and impedance modulus settling around Z_c with increasing frequency. We also found that wave reflections already begin to exert subtle effects on central pressure and flow as early as ~30 milliseconds into systole in the clinical sample. It is worth noting that this timing precedes time of peak aortic flow and the inflection point observed on the aortic pressure waveforms, as supported by previous studies that utilized invasive measurements[24,26,47-49] (discussed in more detail in Data S2). Consistent with these invasive studies, we demonstrate that when the timing of arterial wave reflections is assessed using pressure and flow measurements along with a suitable arterial system model, there is neither theoretical support for a reflectionless state until the time of peak flow nor a need to make such an assumption.

$RWTT_{WSA}$ is a more reliable method than T_{INF} because of its reliance on both pressure and flow data, leading to anticipated relationships with age in the setting of increased PWV. However, this method does not implicitly model the phase shift associated with wave reflections, producing higher absolute values for RWTT and longer values for ERD than the TL modeling, as discussed in Data S2 (Figures S4 and S5). Whereas both TL and WSA demonstrated a reduction of RWTT and the lack of a distal shift of reflection sites with aging, absolute values of RWTT were different. This is not surprising and is explained by the fact that WSA assumes a uniform tube terminated in a pure resistance (as is also the case for T_{INF}), whereas TL does not make this restrictive assumption

because it can model complex and frequency-dependent reflection coefficients as encountered in vivo. A uniform tube terminated in a pure resistance emerges only as a special case of TL if there exists no physical vascular compliance or wave transmission outside the aorta. WSA is therefore unable to capture changes in the complex part of reflection coefficients (which captures physical vascular compliance and pulse wave transmission beyond the aorta). TL emerges as the most robust and physiologic model to assess RWTT.

Despite the differences between WSA and TL modeling, findings from both methods are inconsistent with the previously proposed paradigm[10,11] regarding age-related impedance matching of central-to-peripheral arteries and distal shifting of reflection sites. The motivation for this paradigm was based on a flawed method for reflection timing (T_{INF}) along with the untenable assumption that "PWV matching" is equivalent to impedance matching (Figure S6). The amount of reflection at a given interface (due to conditions downstream) is dependent on the relationship between characteristic impedance of the parent vessel and the complex input impedance of the distal system, rather than being dependent on the relationship between the proximal and distal PWV.[16] The interpretation that matching of carotid-femoral and carotid-brachial PWV denotes impedance matching is inappropriate because it neglects the strong effects of arterial size on wave reflections at the interfaces of elastic and muscular arteries. Furthermore, this interpretation is overly simplistic and does not account for the innumerable sources of wave reflections present in vivo at multiple points of the arterial tree and the complex nature of the input impedance at various arterial beds supplied by individual muscular arteries.[45]

The paradigm of a distal shift of wave reflections has been extended to suggest a "protective" role of reflections at single interfaces between large and muscular arteries that supply target organs (such as the aorta-carotid interface).[50] Mitchell et al proposed that progressive impedance matching at this interface with aging favors the penetration of power to the central nervous system due to a reduction in the local reflection coefficient. This interpretation neglects the fact that impedance matching for forward wave travel in individual first-order bifurcations is already nearly optimized in the natural arterial system because of the anatomical (size) relationship between parent and branch arteries.[45,51] Data reported by Mitchell et al indicate that 95% of the values of reflection coefficients (RC) at this interface across the life span lie in the range of 0% to 15%. Although not reported, it can be readily inferred from standard physics formulas[52-54] that these RCs correspond to power transmission coefficients ($=1-RC^2$) of 97.75% to 100%. Therefore, only a very small proportion (0-2.25%) of power penetration is prevented by this local reflection, in line with the presence of impedance matching at first-order bifurcations across the adult life span in the native arterial system.[40,45,51] In fact, despite its negligible effects on power penetration, positive reflection coefficients at this interface would induce a positive effect on pulse pressure amplification of the transmitted forward-traveling wave.[16,53] More importantly, in contrast to the weak effects of the local reflection on power transmission to the carotid, the effect of innumerable reflections from the lower body produces a substantial composite backward wave, which would penetrate the carotid interface as a forward wave (considerably increasing carotid pulsatile pressure, flow, and power) due to the favorable conditions for forward transmission present at this interface.[45,51] This phenomenon underlies the strong positive (rather than negative) correlation between late systolic carotid pressure and flow augmentation and the concordant increase in carotid pressure and flow augmentation with increasing age.[55]

It should also be noted that, as wave reflections return to the aortic root earlier due to increased PWV, they are re-reflected at the heart and rectified, effectively contributing to (ie, becoming part of) the forward wave independently of aortic root properties.[30,40,51,56,57] Furthermore, the increased pulsatile load from wave reflections has been shown to cause diastolic dysfunction, myocardial hypertrophy, and fibrosis in animal models.[58,59] Similarly, human studies have shown a relationship between wave reflections and worse longitudinal LV function,[60,61] LV hypertrophy,[62] a higher risk of incident new-onset HF,[5,63] and a higher readmission risk after an episode of established acute decompensated HF.[64] Available evidence therefore strongly supports that wave reflections, which arrive earlier to the proximal aorta as PWV increases with aging, are deleterious for target organs, including the heart and the brain.[35,55,65,66] We note that this study did not aim to compare the general population and the clinical samples. Rather, we aimed at assessing prevalent values of RWTT across the adult age spectrum in both the general population and a clinical setting. We demonstrate highly consistent trends with aging in the 2 populations.

Our study should be interpreted in the context of its strengths and limitations. Strengths include consistency of results between both the unselected and clinical cohorts, which supports the generalization of the TL model previously validated in animals.[24,31] Furthermore, in contrast to the studies that use left ventricular outflow tract flow as a surrogate of aortic flow,[10,39] our study uses ascending aortic flow, which more closely obeys the requirements for assessing aortic input impedance.[35,40,41,67] Limitations of our study include the use of carotid tonometry to obtain a surrogate of aortic pressure, which carries some potential for operator dependency. However, this technique is widely accepted for central hemodynamic assessment[68] and is the same technique used in a number of human population studies.[7,35,39]

Whereas each of the 2 substudies included a wide age range of age (~4 decades), with an overall span of ~5 decades, the addition of younger individuals to the clinical sample and older individuals to the general sample would have strengthened our study. The TL model employed is necessarily a reduced representation of the arterial system that does not inform on regional aortic stiffening/dilation; identification of regional changes that occur with aging would require a more complex and validated model (eg, modified asymmetric T-tube[26]) and should be a focus for future studies.

Perspectives

In contrast to studies that relied on T_{INF}, the application of appropriate methods based on pressure-flow analyses demonstrates that increased PWV with aging is associated with an earlier arrival of wave reflections at the proximal aorta, without a distal shift of reflecting sites. Our findings reconcile the apparent paradox introduced by misinterpretation of T_{INF} as a surrogate of RWTT, which is incompatible with standard hemodynamic theory and falsely suggests a distal shift in reflection sites. The assumption that "impedance matching" leads to a distal shift in reflection sites is therefore disproven. Wave reflections arriving earlier to the proximal aorta as PWV increases with aging are deleterious for target organs, including the heart and the brain. Strategies at reducing early wave reflections should be tested as a potential strategy to reduce the burden of cardiovascular disease in older age.

Sources of Funding

This research was funded by NIH grants R56 HL-124073-01A1 (Chirinos), 5-R21-AG-043802-02 (Chirinos), and PPG: 1P01-1HL094307 (Pack).

Disclosures

Dr Chirinos is a consultant to Bristol-Myers Squibb, OPKO Healthcare, Fukuda Denshi, Microsoft, and Merck. He received research grants from National Institutes of Health, American College of Radiology Imaging Network, Fukuda Denshi, Bristol-Myers Squibb, Microsoft, and CVRx Inc, and a device loan from AtCor Medical. He is named as inventor in a University of Pennsylvania patent application for the use of inorganic nitrates/nitrites for the treatment of Heart Failure and Preserved Ejection Fraction. The other authors do not have any disclosures.

References

1. Franklin SS, Gustin W, Wong ND, Larson MG, Weber MA, Kannel WB, Levy D. Hemodynamic patterns of age-related changes in blood pressure: the Framingham Heart Study. *Circulation*. 1997;96:308–315.
2. Willum Hansen T. Prognostic value of aortic pulse wave velocity as index of arterial stiffness in the general population. *Circulation*. 2006;113:664–670.
3. Namasivayam M, McDonnell BJ, McEniery CM, O'Rourke MF; on behalf of the Anglo-Cardiff Collaborative Trial Study Investigators. Does wave reflection dominate age-related change in aortic blood pressure across the human life span? *Hypertension*. 2009;53:979–985.
4. Manisty C, Mayet J, Tapp RJ, Parker KH, Sever P, Poulter NH, Thom SAM, Hughes AD. Wave reflection predicts cardiovascular events in hypertensive individuals independent of blood pressure and other cardiovascular risk factors. *J Am Coll Cardiol*. 2010;56:24–30.
5. Chirinos JA, Kips JG, Jacobs DR, Brumback L, Duprez DA, Kronmal R, Bluemke DA, Townsend RR, Vermeersch S, Segers P. Arterial wave reflections and incident cardiovascular events and heart failure. *J Am Coll Cardiol*. 2012;60:2170–2177.
6. Townsend RR, Wilkinson IB, Schiffrin EL, Avolio AP, Chirinos JA, Cockcroft JR, Heffernan KS, Lakatta EG, McEniery CM, Mitchell GF, Najjar SS, Nichols WW, Urbina EM, Weber T. Recommendations for improving and standardizing vascular research on arterial stiffness: a scientific statement from the American Heart Association. *Hypertension*. 2015;66:698–722.
7. Mitchell GF, Wang N, Palmisano JN, Larson MG, Hamburg NM, Vita JA, Levy D, Benjamin EJ, Vasan RS. Hemodynamic correlates of blood pressure across the adult age spectrum: noninvasive evaluation in the Framingham Heart Study. *Circulation*. 2010;122:1379–1386.
8. Izzo JL. Brachial vs. central systolic pressure and pulse wave transmission indicators: a critical analysis. *Am J Hypertens*. 2014;27:1433–1442.
9. O'Rourke MF, Nichols WW. Aortic diameter, aortic stiffness, and wave reflection increase with age and isolated systolic hypertension. *Hypertension*. 2005;45:652–658.
10. Mitchell GF, Parise H, Benjamin EJ, Larson MG, Keyes MJ, Vita JA, Vasan RS, Levy D. Changes in arterial stiffness and wave reflection with advancing age in healthy men and women: the Framingham Heart Study. *Hypertension*. 2004;43:1239–1245.
11. Torjesen AA, Wang N, Larson MG, Hamburg NM, Vita JA, Levy D, Benjamin EJ, Vasan RS, Mitchell GF. Forward and backward wave morphology and central pressure augmentation in men and women in the Framingham Heart Study. *Hypertension*. 2014;64:259–265.
12. Sugawara J, Hayashi K, Tanaka H. Distal shift of arterial pressure wave reflection sites with aging. *Hypertension*. 2010;56:920–925.
13. Baksi AJ, Treibel TA, Davies JE, Hadjiloizou N, Foale RA, Parker KH, Francis DP, Mayet J, Hughes AD. A meta-analysis of the mechanism of blood pressure change with aging. *J Am Coll Cardiol*. 2009;54:2087–2092.
14. Schultz MG, Davies JE, Sharman JE. Central blood pressure physiology: a (more) critical analysis. *Am J Hypertens*. 2015;28:690–691.
15. Izzo JL. Response to "Central Blood Pressure Physiology" a (more) critical review (Schultz et al.). *Am J Hypertens*. 2015;28:692.
16. Westerhof N, Westerhof BE. Wave transmission and reflection of waves: "The myth is in their use". *Artery Res*. 2012;6:1–6.
17. Segers P, Rietzschel ER, De Buyzere ML, De Bacquer D, Van Bortel LM, De Backer G, Gillebert TC, Verdonck PR. Assessment of pressure wave reflection: getting the timing right! *Physiol Meas*. 2007;28:1045–1056.
18. Westerhof BE, Westerhof N. Magnitude and return time of the reflected wave: the effects of large artery stiffness and aortic geometry. *J Hypertens*. 2012;30:932–939.
19. Karamanoglu M, Feneley MP. Late systolic pressure augmentation: role of left ventricular outflow patterns. *Am J Physiol Heart Circ Physiol*. 1999;277:H481–H487.
20. Sharman JE, Davies JE, Jenkins C, Marwick TH. Augmentation index, left ventricular contractility, and wave reflection. *Hypertension*. 2009;54:1099–1105.
21. Heiberg E, Sjögren J, Ugander M, Carlsson M, Engblom H, Arheden H. Design and validation of segment—freely available software for cardiovascular image analysis. *BMC Med Imaging*. 2010;10:1.
22. Westerhof N, Sipkema P, Bos GCVD, Elzinga G. Forward and backward waves in the arterial system. *Cardiovasc Res*. 1972;6:648–656.
23. Cholley BP, Lang RM, Berger DS, Korcarz C, Payen D, Shroff SG. Alterations in systemic arterial mechanical properties during septic shock: role of fluid resuscitation. *Am J Physiol*. 1995;269:H375–H384.
24. Burattini R, Di Carlo S. Effective length of the arterial circulation determined in the dog by aid of a model of the systemic input impedance. *IEEE Trans Biomed Eng*. 1988;35:53–61.
25. Berger DS, Robinson KA, Shroff SG. Wave propagation in coupled left ventricle arterial system: implications for aortic pressure. *Hypertension*. 1996;27:1079–1089.

26. Burattini R, Campbell KB. Modified asymmetric T-tube model to infer arterial wave reflection at the aortic root. *IEEE Trans Biomed Eng*. 1989;36:805–814.
27. Burattini R, Knowlen GG, Campbell KB. Two arterial effective reflecting sites may appear as one to the heart. *Circ Res*. 1991;68:85–99.
28. Berger DS, Li JK, Noordergraaf A. Differential effects of wave reflections and peripheral resistance on aortic blood pressure: a model-based study. *Am J Physiol Heart Circ Physiol*. 1994;266:H1626–H1642.
29. Poppas A, Shroff SG, Korcarz CE, Hibbard JU, Berger DS, Lindheimer MD, Lang RM. Serial assessment of the cardiovascular system in normal pregnancy: role of arterial compliance and pulsatile arterial load. *Circulation*. 1997;95:2407–2415.
30. Phan TS, Li JK, Segers P, Chirinos JA. Misinterpretation of the determinants of elevated forward wave amplitude inflates the role of the proximal aorta. *J Am Heart Assoc*. 2016;5:e003069 doi: 10.1161/JAHA.115.003069.
31. Burattini R, Campbell KB. Physiological relevance of uniform elastic tube-models to infer descending aortic wave reflection: a problem of identifiability. *Ann Biomed Eng*. 2000;28:512–523.
32. Bos GCVD, Westerhof N, Elzinga G, Sipkema P. Reflection in the systemic arterial system: effects of aortic and carotid occlusion. *Cardiovasc Res*. 1976;10:565–573.
33. Murgo JP, Westerhof N, Giolma JP, Altobelli SA. Aortic input impedance in normal man: relationship to pressure wave forms. *Circulation*. 1980;62:105–116.
34. Safar ME, O'Rourke MF. The brachial–ankle pulse wave velocity. *J Hypertens*. 2009;27:1960–1961.
35. Nichols WW, Nichols WW, McDonald DA, eds. *McDonald's Blood Flow in Arteries: Theoretic, Experimental, and Clinical Principles*. 6th ed. London: Hodder Arnold; 2011.
36. Sipkema P, Westerhof N. Effective length of the arterial system. *Ann Biomed Eng*. 1975;3:296–307.
37. Mitchell GF, Hwang S-J, Vasan RS, Larson MG, Pencina MJ, Hamburg NM, Vita JA, Levy D, Benjamin EJ. Arterial stiffness and cardiovascular events: the Framingham Heart Study. *Circulation*. 2010;121:505–511.
38. Yin FCP. Aging and vascular impedance. In: Yin FCP, ed. *Ventricular/Vascular Coupling*. New York, NY: Springer; 1987:115–139.
39. Segers P, Rietzschel ER, De Buyzere ML, Vermeersch SJ, De Bacquer D, Van Bortel LM, De Backer G, Gillebert TC, Verdonck PR; on behalf of the Asklepios investigators. Noninvasive (input) impedance, pulse wave velocity, and wave reflection in healthy middle-aged men and women. *Hypertension*. 2007;49:1248–1255.
40. Milnor WR. *Hemodynamics*. 2nd ed. Baltimore, MD: Williams & Wilkins; 1989.
41. Westerhof N, Stergiopulos N, Noble MIM. *Snapshots of Hemodynamics an Aid for Clinical Research and Graduate Education*. New York, NY: Springer; 2010.
42. O'Rourke MF. Pressure and flow waves in systemic arteries and the anatomical design of the arterial system. *J Appl Physiol*. 1967;23:139–149.
43. Burattini R. Downstream from the heart left ventricle. In: Carson E ,Cobelli C, ed. *Modelling Methodology for Physiology and Medicine, 2nd Ed*. London: Elsevier; 2014:503–525.
44. Milnor WR, Bertram CD. The relation between arterial viscoelasticity and wave propagation in the canine femoral artery in vivo. *Circ Res*. 1978;43:870–879.
45. Li JK, Melbin J, Noordergraaf A. Directional disparity of pulse reflection in the dog. *Am J Physiol Heart Circ Physiol*. 1984;247:H95–H99.
46. Li JK, Melbin J, Riffle RA, Noordergraaf A. Pulse wave propagation. *Circ Res*. 1981;49:442–452.
47. Burattini R, Gnudi G. Computer identification of models for the arterial tree input impedance: comparison between two new simple models and first experimental results. *Med Biol Eng Comput*. 1982;20:134–144.
48. Shroff SG, Berger DS, Korcarz C, Lang RM, Marcus RH, Miller DE. Physiological relevance of T-tube model parameters with emphasis on arterial compliances. *Am J Physiol*. 1995;269:H365–H374.
49. Phan TS, Londono F, Chirinos JA, Li JK-J. Augmentation index is blind to early-systolic effects of arterial wave reflections. *J Am Soc Hypertens*. 2016;10:e34.
50. Mitchell GF, van Buchem MA, Sigurdsson S, Gotal JD, Jonsdottir MK, Kjartansson O, Garcia M, Aspelund T, Harris TB, Gudnason V, Launer LJ. Arterial stiffness, pressure and flow pulsatility and brain structure and function: the Age, Gene/Environment Susceptibility—Reykjavik Study. *Brain*. 2011;134:3398–3407.
51. Noordergraaf A. *Blood in Motion*. New York, NY: Springer; 2011.
52. Orfanidis SJ. *Electromagnetic Waves and Antennas*. New Brunswick, NJ: Rutgers University; 2002.
53. Paul CR. *Analysis of Multiconductor Transmission Lines*. Hoboken, NJ: Wiley-Interscience; 2008.
54. Oates C. *Cardiovascular Haemodynamics and Doppler Waveforms Explained*. New York, NY: Cambridge University Press; 2001.
55. Hirata K, Yaginuma T, O'Rourke MF, Kawakami M. Age-related changes in carotid artery flow and pressure pulses: possible implications for cerebral microvascular disease. *Stroke*. 2006;37:2552–2556.
56. Noordergraaf A. Hemodynamics. In: Schwan HP, ed. *Biological Engineering*. New York, NY: McGraw-Hill; 1969:391–545.
57. Berger DS, Li JK, Laskey WK, Noordergraaf A. Repeated reflection of waves in the systemic arterial system. *Am J Physiol*. 1993;264:H269–H281.
58. Kobayashi S, Yano M, Kohno M, Obayashi M, Hisamatsu Y, Ryoke T, Ohkusa T, Yamakawa K, Matsuzaki M. Influence of aortic impedance on the development of pressure-overload left ventricular hypertrophy in rats. *Circulation*. 1996;94:3362–3368.
59. Gillebert TC, Lew WY. Influence of systolic pressure profile on rate of left ventricular pressure fall. *Am J Physiol*. 1991;261:H805–H813.
60. Chirinos JA, Segers P, Rietzschel ER, De Buyzere ML, Raja MW, Claessens T, De Bacquer D, St John Sutton M, Gillebert TC; Asklepios Investigators. Early and late systolic wall stress differentially relate to myocardial contraction and relaxation in middle-aged adults: the Asklepios study. *Hypertension*. 2013;61:296–303.
61. Chirinos JA, Segers P, Gillebert TC, Gupta AK, De Buyzere ML, De Bacquer D, St John-Sutton M, Rietzschel ER; on behalf of the Asklepios Investigators. Arterial properties as determinants of time-varying myocardial stress in humans. *Hypertension*. 2012;60:64–70.
62. Hashimoto J, Westerhof BE, Westerhof N, Imai Y, O'Rourke MF. Different role of wave reflection magnitude and timing on left ventricular mass reduction during antihypertensive treatment. *J Hypertens*. 2008;26:1017–1024.
63. Shah SJ, Wasserstrom JA. Increased arterial wave reflection magnitude: a novel form of stage B heart failure? *J Am Coll Cardiol*. 2012;60:2178–2181.
64. Sung S-H, Yu W-C, Cheng H-M, Lee C-W, Lin M-M, Chuang S-Y, Chen C-H. Excessive wave reflections on admission predict post-discharge events in patients hospitalized due to acute heart failure. *Eur J Heart Fail*. 2012;14:1348–1355.
65. O'Rourke MF, Safar ME. Relationship between aortic stiffening and microvascular disease in brain and kidney: cause and logic of therapy. *Hypertension*. 2005;46:200–204.
66. Coutinho T, Turner ST, Kullo IJ. Aortic pulse wave velocity is associated with measures of subclinical target organ damage. *JACC Cardiovasc Imaging*. 2011;4:754–761.
67. Noordergraaf A. *Circulatory System Dynamics*. New York, NY: Academic Press; 1978.
68. Kelly R, Fitchett D. Noninvasive determination of aortic input impedance and external left ventricular power output: a validation and repeatability study of a new technique. *J Am Coll Cardiol*. 1992;20:952–963.

SUPPLEMENTAL MATERIAL

Data S1. Supplemental Methods

Input Impedance of Uniform Tube Models[1]

Model A. Uniform Elastic Tube with a Resistive Load

Input impedance of this model is expressed in its most general form as

$$Z_{in,INF}(j\omega) = Z_c \frac{1+\Gamma_{L,A}(j\omega)e^{-j2\omega\tau_A}}{1-\Gamma_{L,A}(j\omega)e^{-j2\omega\tau_A}} \quad (1)$$

where Z_c is characteristic impedance of the tube and τ_A is the one-way wave transit time to the reflection site at the terminal end of the tube.

$\Gamma_{L,A}(j\omega)$ is the load reflection coefficient seen at the termination, where $Z_L(j\omega)$ is the terminal load impedance:

$$\Gamma_{L,A}(j\omega) = \frac{Z_{L,A}(j\omega)-Z_c}{Z_{L,A}(j\omega)+Z_c} \quad (2)$$

In the case of a purely resistive load, the load impedance $Z_L(j\omega)$ is frequency-independent and is simply equal to total peripheral resistance R_p. This reduces the load reflection coefficient to a purely real number in the mathematical sense (i.e. frequency-independent).

$$\Gamma_{L,A} = \frac{R_p-Z_c}{R_p+Z_c} \quad (3)$$

Input impedance can then be expressed in its final form:

$$Z_{in,INF}(j\omega) = Z_c \frac{1+\Gamma_{L,A}e^{-j2\omega\tau_A}}{1-\Gamma_{L,A}e^{-j2\omega\tau_A}} \quad (4)$$

With values of three parameters $\{R_p, Z_c, \tau_A\}$, a continuous input impedance spectrum can be obtained.

In the case of time to inflection point on the pressure waveform (T_{INF}), τ_A is one half this value, $\tau_A = 0.5*T_{INF.}$ Z_c is characteristic impedance of the aorta, estimated from pressure-flow data using standard methods, and R_p is the ratio of mean arterial pressure to cardiac output.

Use of the quarter wavelength formula to estimate "effective length" (L_{eff}) of the arterial system or equivalently, "effective reflection distance" (ERD), assumes this particular input impedance model, where PWV is pulse wave velocity and f_{min} is the frequency at the first minimum of the impedance modulus.[2]

$$L_{eff,INF} = ERD_{INF} = \frac{PWV}{4\,f_{min}} \quad (5)$$

In this model, the first zero-crossing of impedance phase occurs at the same frequency (f_{zc}) as f_{min}.

Since use of equation (5) requires both pressure and flow waveforms to determine f_{min} (impedance analysis), attempts have been made to determine a surrogate of f_{min} from analysis of the pressure waveform alone (i.e. T_{INF}). It has been reported that T_{INF} determined from analysis

of the pressure waveform alone correlates well to f_{min} from impedance data, such that the following relation can be substituted for f_{min}[3,4]:

$$f_{min} = 1/(2T_{INF})$$

Upon substitution into equation (5), this leads to the commonly used equation for effective reflection distance, using pressure-waveform-only analysis along with a measurement of PWV:

$$L_{eff,INF} = ERD_{INF} = \frac{PWV}{2} T_{INF} \quad (6)$$

The reported high correlation between T_{INF} and f_{min} is important so long as the input impedance implied by the underlying model can suitably approximate measured arterial input impedance. Figure S2A shows input impedance implied by this model for each decade of age in the healthy aging sample.

It can be appreciated that there are strong dissimilarities with patterns of reported arterial input impedance in the literature.[2,4,5] Note the strong oscillation in the impedance modulus plot. This would indicate very strong reflections in the higher frequencies, which is inconsistent with patterns encountered *in vivo*. Furthermore, the phase angle of Figure S2A oscillates strongly between very negative to very positive values.

Model B. Uniform Elastic Tube with a (Complex) Frequency-Dependent Load

In order to better match the classical tube models to the complex and frequency-dependent reflection coefficients encountered *in vivo*, a terminal load that accounts for the low-pass filtering features of the distal circulation can be incorporated.[6]

Load impedance can then be expressed in terms of R_p, load compliance (C_l), and a high-frequency resistive element (R_d). Input impedance of this model ($Z_{in,B}$) can be made to match aortic Z_c with increasing frequency, as encountered *in vivo*, if R_d is expressed as follows:

$$R_d = \frac{R_p Z_c}{R_p - Z_c} \quad (7)$$

Load impedance of this model, $Z_{L,B}(j\omega)$ is expressed as

$$Z_{L,B}(j\omega) = R_p \frac{1+j\omega\tau_n}{1+j\omega\tau_d} \quad (8)$$

where the time constants (τ_n, τ_d) are defined as

$$\tau_n = R_d C_l$$
$$\tau_d = (R_p + R_d) C_l$$

The reflection coefficient seen at load is thus frequency-dependent

$$\Gamma_{L,B}(j\omega) = \frac{Z_{L,B}(j\omega) - Z_c}{Z_{L,B}(j\omega) + Z_c} \quad (9)$$

and input impedance of this model can be fully expressed as

$$Z_{in,TL}(j\omega) = Z_c \frac{1+\Gamma_{L,B}(j\omega)e^{-j2\omega\tau_B}}{1-\Gamma_{L,B}(j\omega)e^{-j2\omega\tau_B}} \quad (10)$$

τ_B is the one-way wave transit time to the reflection site in this model, equal to one half of $RWTT_{TL}$ used in the current study.

ERD can then be calculated as

$$L_{eff,TL} = ERD_{TL} = PWV * \tau_B = PWV \frac{RWTT_{TL}}{2} \quad (11)$$

Figure S2B shows input impedance implied by this model for each decade of age in the healthy aging sample. These patterns resemble much more closely the reported arterial input impedance patterns with aging.[2,4,5,7,8]

Data S2. Supplemental Discussion

Quarter Wavelength Formula Overestimates Effective Reflection Distance

As clarified by Burattini *et al*[6,9,10], when the effective reflection site is more suitably represented by a complex reflection coefficient, the ERD can be computed as $ERD = \frac{PWV}{4\, f_{zc}}\left(1 + \frac{\vartheta(f_{zc})}{\pi}\right)$, where f_{zc} is the frequency at which the input impedance angle crosses zero and $\upsilon(f_{zc})$ is the phase of the effective (load) reflection coefficient at frequency of f_{zc}; note that the quarter wavelength formula emerges when $\upsilon(f_{zc})$ is set to zero. Because the phase of reflection [$\upsilon(f_{zc})$] is generally negative *in vivo*[9,11–13], ERD calculations that account for the phase of reflection will necessarily be less than values computed by the quarter wavelength formula. This explains why the frequently reported values of ERD employing the quarter wavelength formula[4,14,15,5,16] are significantly higher than values we report here using tube-load modeling. The general acceptance and frequent reporting of ERD estimates[5,17] of around 0.5 m computed by the quarter wavelength formula may indeed be consensus-based (since 0.5 m from the heart is close to the terminal aortic bifurcation and apparently plausible) rather than on appropriate use of a suitable reduced model of the arterial system.

Early-Systolic (Before Peak Flow) Reflections

In regards to the apparent reflection-free early-systole implied by T_{INF}, the hemodynamic literature provides support for the existence of early-systolic effects of wave reflections. In a study of seven mongrel dogs in which invasive and simultaneous measurements of aortic pressure and flow were analyzed[6], Burattini and Di Carlo found that one-way wave transit times (to an effective reflection site) averaged 14 msec (calculated as $\sqrt{(ld)(cd)}$ from their Table I), giving a $RWTT_{TL}$ of 28 msec. This timing precedes time of peak flow and the inflection point observed on the aortic pressure waveforms, which occurred around 50 msec. In another study combining a large-scale model of the systemic arterial tree based on Womersley's theory and dog experiments, $RWTT_{TL}$ averaged 37.2 msec.[18] Although the studies employed the same tube-load model we use in the present study (for estimating $RWTT_{TL}$), it can be appreciated that both their invasive and numerical and our noninvasive studies agree that significant effects of reflection can precede time of peak flow (and T_{INF}).

With the additional measurement of descending thoracic aortic flow, studies of wave reflection can be extended to the modified asymmetric T-tube model.[19] Applying this model to dogs, Shroff et al.[20] found one-way transit times to effective reflection sites in the head-end and body-end circulations of approximately 25 msec and 55 msec, respectively, during control conditions; peak flow occurred around 60 msec and calculated RWTT from the head-end circulation (~50 msec) preceded peak flow. Burattini and Campbell, applying the same model, similarly found times of 26.5 msec and 68.5 msec for head-end and body-end circulations, with peak flow similarly occurring at around 60 msec. Consistent with these invasive studies, when the timing of arterial wave reflections is assessed using both pressure and flow measurements (as opposed to pressure-only analysis), along with a suitable arterial system model, there is no theoretical support for a reflection-less state until the time of peak, nor there is a need to make this assumption.

Reports evaluating time-domain techniques to estimate aortic characteristic impedance from early-systolic pressure-flow relationships also lend support for reflections that can occur prior to time of peak flow.[21,22] Estimations of aortic Z_c vary depending on the region chosen on the early-systolic pressure-flow waveforms, with various authors invoking different criteria to minimize the effects of reflections (e.g. first 60 msec of ejection, period up to 95% of peak flow, peak derivatives, etc.).[23–25] Evidence of early-systolic wave reflections have also been found when estimating local pulse wave velocity in both *in vivo* and in 3D fluid-structure interaction simulation studies.[26,27] It was shown that an apparent linear early-systolic relation between pressure and flow (velocity) is insufficient to conclude a reflection-free period in early-systole; wave reflections can cause under- and over-estimation of local pulse wave velocity. Therefore, applying methods that purportedly track timing of wave reflections but are apparently blind to early-systolic wave reflections should be discouraged, since they lead to artificial asymptotes when studied across a large range of age.

Modeling Study: $RWTT_{WSA}/ERD_{WSA}$ Confounded by the Phase of Reflection

We note that the pattern of changes in $RWTT_{WSA}$ with aging roughly parallels that of $RWTT_{TL}$ across the age spectrum studied. We conducted a modeling study (below), which confirmed that the apparent discrepancy in absolute RWTT values is due to the fact that $RWTT_{WSA}$ does not account for complex nature of the reflection coefficient (i.e. frequency-dependent in magnitude and phase) encountered *in vivo*, whereas tube-load modeling implicitly does. Therefore, time delay measures between P_f and P_b represent an accurate estimate of RWTT if phase shifts at the reflection site are assumed to be absent. $RWTT_{TL}$ emerges as the most logically consistent and theoretically justifiable measure of RWTT.

A model of the left ventricle[28,29] (LV) coupled to the aorta terminating in a complex load[6] was used to demonstrate the effects of the phase of reflection on $RWTT_{WSA}$ and ERD_{WSA}. This model incorporates a single (complex) reflecting site at a known distance from the heart (28 cm).

The parameters characterizing the LV model: E_{max} = 1.53 mmHg•mL^{-1}; E_{min} = 0.08 mmHg•mL^{-1}; EDV = 157 mL; HR = 75 bpm; k = 0.0005 s•mL^{-1}.

The parameters used in the arterial system model: PWV = 700 $cm \bullet s^{-1}$; d = 28 cm; Z_0 = 0.079 $mmHg \bullet s \bullet mL^{-1}$; R_p = 0.85 $mmHg \bullet s \bullet mL^{-1}$; C = 1.21 $mL \bullet mmHg^{-1}$.

Aortic input impedance of the model is shown in Figure S4. The vertical red line indicates the frequency of the impedance modulus minimum. The vertical purple line indicates the frequency at which the phase crosses zero. Consistent with impedance patterns observed *in vivo*, these two frequencies are not identical.[6,30]

Aortic pressure and flow waveforms from the model are shown in Figure S5A. After wave separation analysis, the forward and backward pressure waves are shown in Figure S5B. The dashed vertical red and green lines indicate the zero-crossings of the backward and forward pressure waves, respectively.

$RWTT_{WSA}$ was calculated as 160 msec and with use of the known PWV=700 cm/s, ERD_{WSA} is estimated as 56 cm. In this case, length of the aorta is overestimated by 100% (known length of the aorta is 28 cm), due to the phase shift caused by reflection at the complex load. This is the same limitation encountered by using T_{INF} as reflection timing; $RWTT_{WSA}$ and T_{INF} will provide accurate estimates of reflection timing only if reflection coefficients encountered *in vivo* are purely real (e.g. that vascular compliance and wave transmission phenomena are non-existent outside the aorta). It is interesting to note that the overestimation of ERD by ERD_{WSA} of this example is on the same order of magnitude observed in the younger adults of the present study (Figure 2); accounting for the different phases of reflection for each subject, as implicit in the $RWTT_{TL}$ and ERD_{TL} procedure used in the present study, resolves the overestimation.

Figure S1. Example of a case in which the zero-crossing of P_b is poorly defined. Due to the the presence of noise, particularly on high-frequency features of pressure and flow waveforms, single-point landmarks (e.g. zero-crossing, 'foot') may be ambiguous. Note that there is no apparent 'foot' to the backward wave (due to the presence of multiple reflection sites *in vivo*). Empirically imposing a 'foot' to P_b may amplify the significance of high-frequency artefacts (e.g. due to pressure-flow alignment processes, use of surrogate waveforms, etc.).

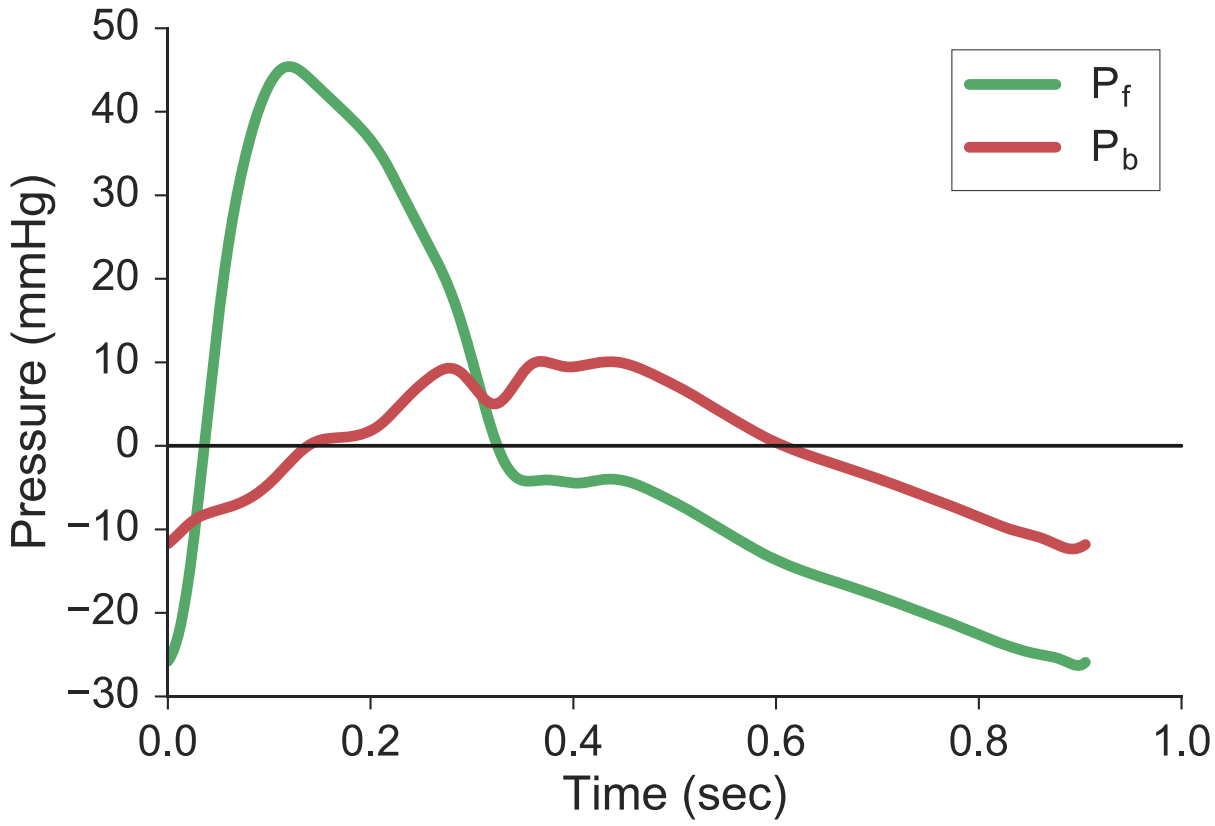

Figure S2. Arterial input impedance implied by (A) T_{INF} and the quarter wavelength formula, and (B) tube-load modeling with a complex and frequency-dependent load for each decade of age in the clinical sample. Vertical lines correspond to the frequencies of impedance modulus minimum and phase angle zero-crossings.

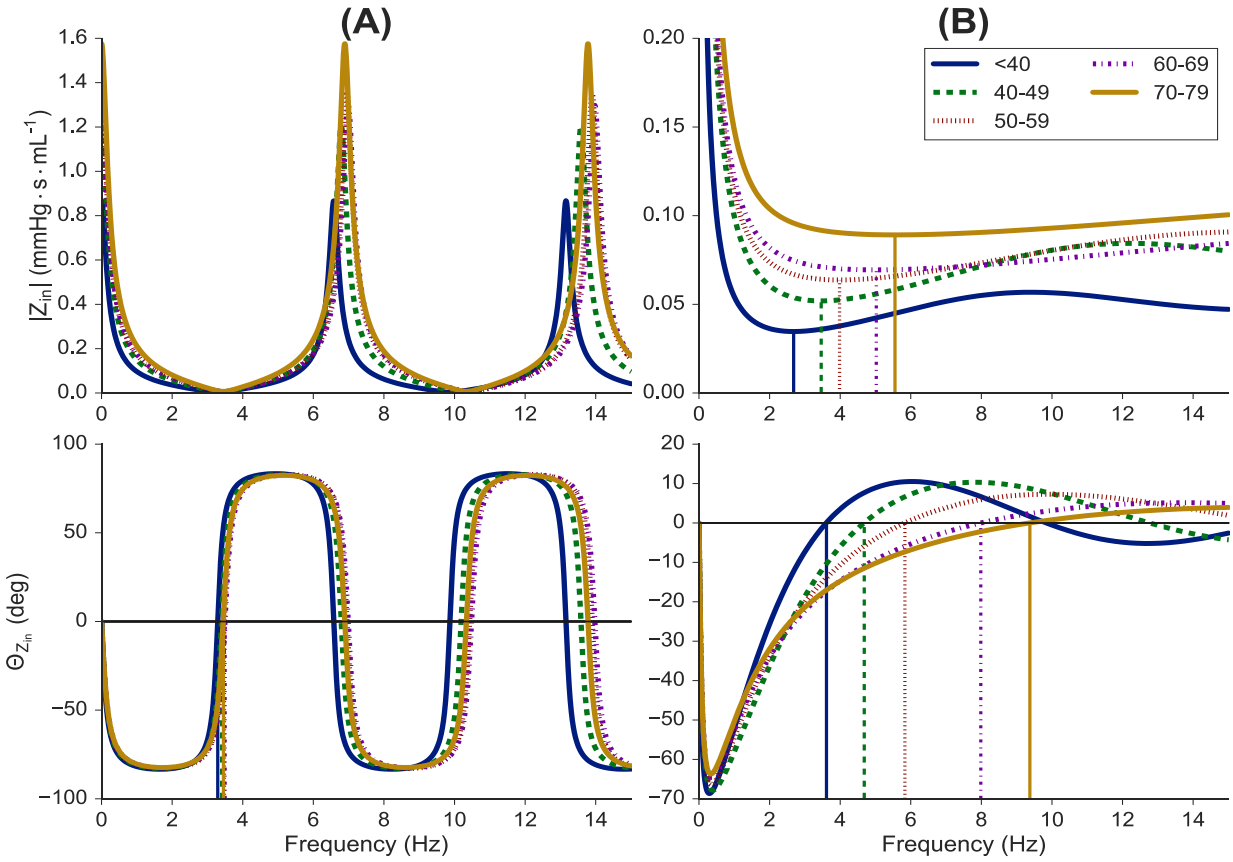

Figure S3. Arterial input impedance implied by (A) T_{INF} and the quarter wavelength formula, and (B) tube-load modeling with a complex and frequency-dependent load for each decade of age in the general sample. Vertical lines correspond to the frequencies of impedance modulus minimum and phase angle zero-crossings.

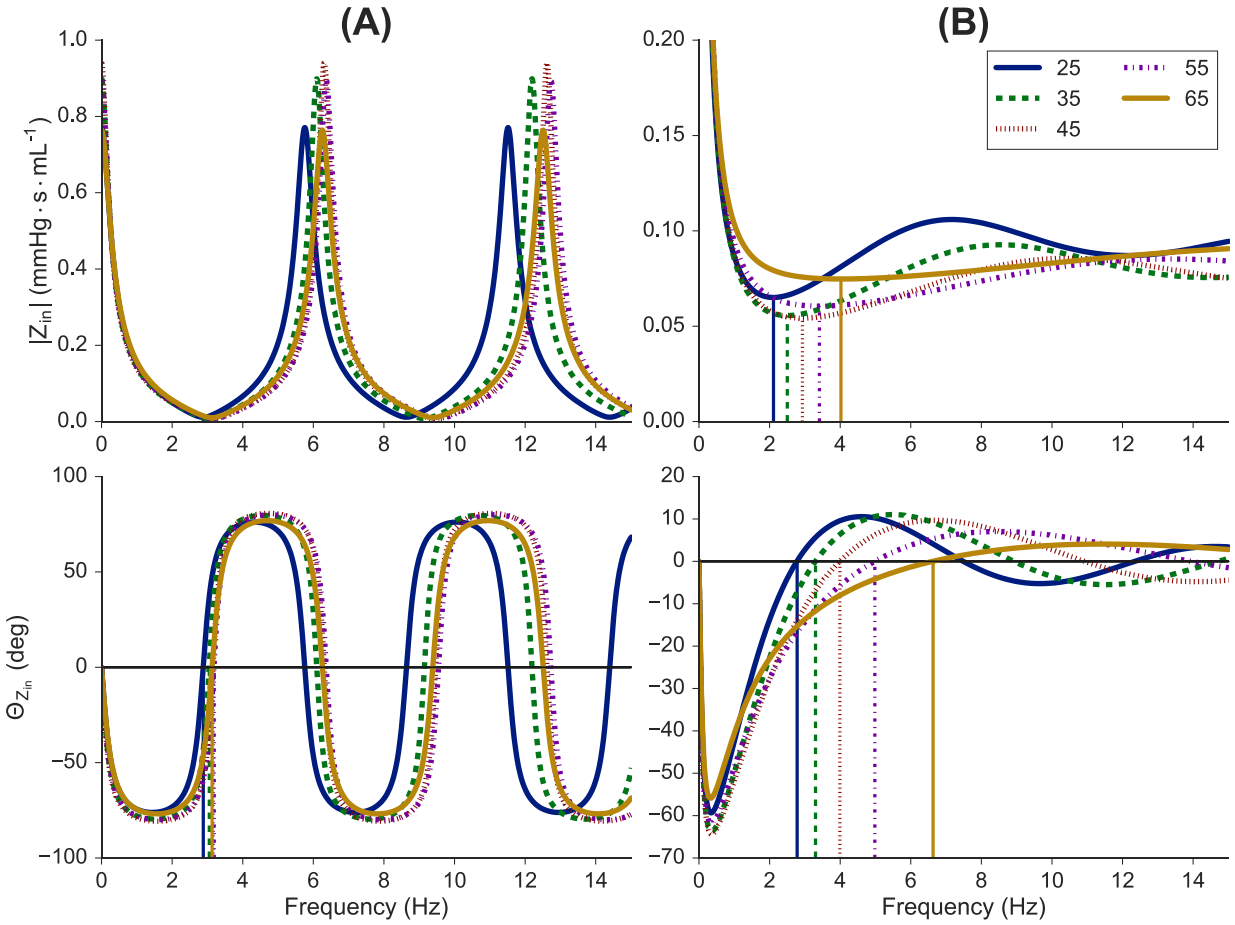

Figure S4. Aortic input impedance from the model-based study. The vertical red and purple lines correspond to the frequencies at which the impedance modulus is minimum and the phase angle crosses zero degrees, respectively. As generally encountered *in vivo*, these two frequencies are not identical.

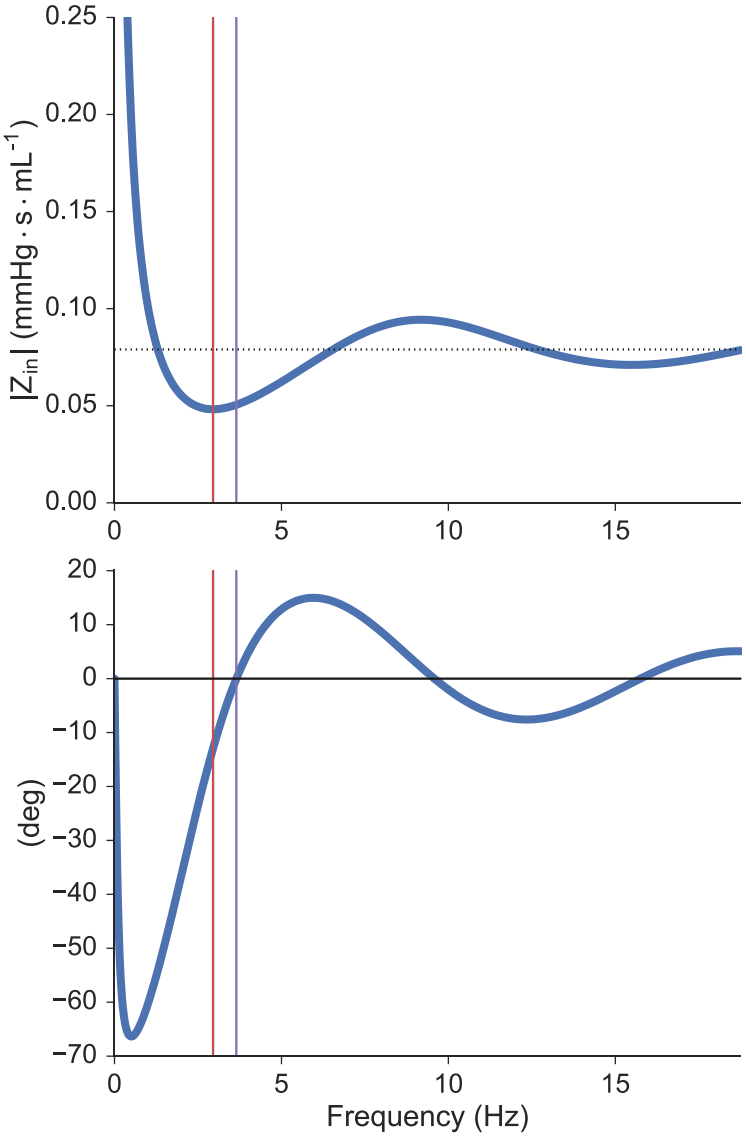

Figure S5. (A) Aortic pressure and flow waveform from the model-based study. (B) Aortic pressure separated into its forward and backward traveling components. The vertical dashed green and red lines correspond to the zero-crossings of the forward and backward waves, respectively.

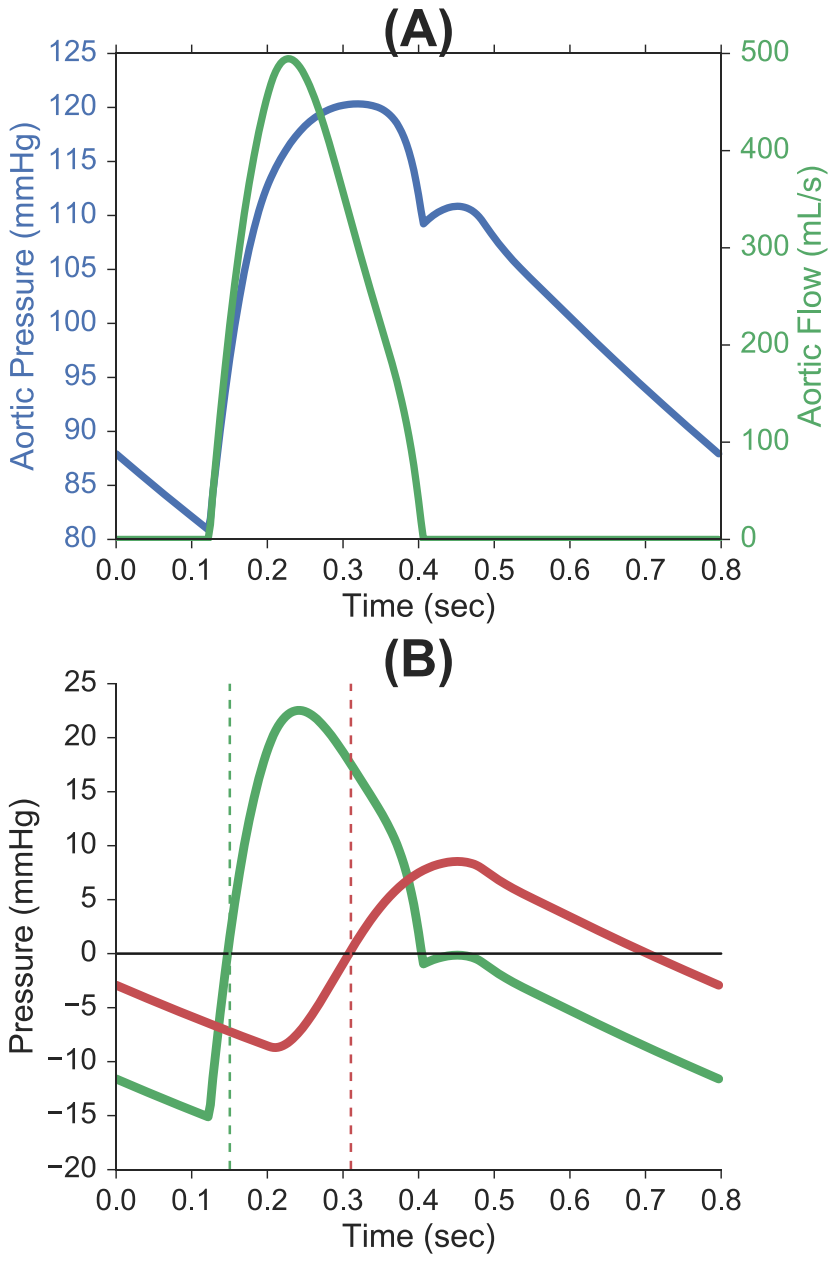

Figure S6. Carotid-radial PWV measurements were available in the clinical population sample. The reported[15] trend of carotid-femoral PWV surpassing muscular artery PWV is reproduced in our clinical sample. Contrary to the age-related impedance-matching interpretation of this PWV-gradient cross-over, pressure-flow analyses reveal earlier effects of reflection.

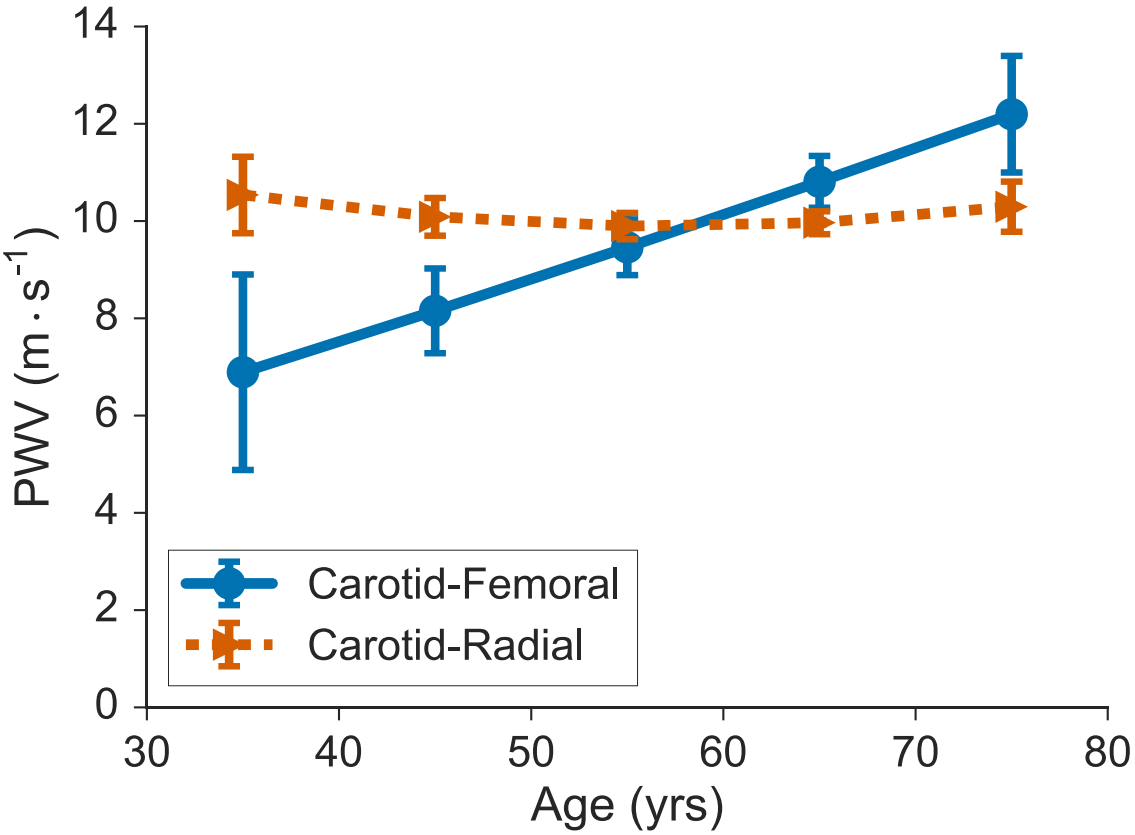

References:

1. Burattini R, Campbell KB. Physiological Relevance of Uniform Elastic Tube-Models to Infer Descending Aortic Wave Reflection: A Problem of Identifiability. *Annals of Biomedical Engineering*. 2000;28:512–523.
2. Latham RD, Westerhof N, Sipkema P, Rubal BJ, Reuderink P, Murgo JP. Regional wave travel and reflections along the human aorta: a study with six simultaneous micromanometric pressures. *Circulation*. 1985;72:1257–1269.
3. Bos GCVD, Westerhof N, Elzinga G, Sipkema P. Reflection in the systemic arterial system: effects of aortic and carotid occlusion. *Cardiovascular Research*. 1976;10:565–573.
4. Murgo JP, Westerhof N, Giolma JP, Altobelli SA. Aortic input impedance in normal man: relationship to pressure wave forms. *Circulation*. 1980;62:105–116.
5. Nichols WW, Nichols WW, McDonald DA eds. *McDonald's blood flow in arteries: theoretic, experimental, and clinical principles*. 6th ed. London: Hodder Arnold; 2011.
6. Burattini R, Di Carlo S. Effective length of the arterial circulation determined in the dog by aid of a model of the systemic input impedance. *IEEE Transactions on Biomedical Engineering*. 1988;35:53–61.
7. Kelly R, Fitchett D. Noninvasive determination of aortic input impedance and external left ventricular power output: A validation and repeatability study of a new technique. *Journal of the American College of Cardiology*. 1992;20:952–963.
8. Segers P, Rietzschel ER, De Buyzere ML, Vermeersch SJ, De Bacquer D, Van Bortel LM, De Backer G, Gillebert TC, Verdonck PR, on behalf of the Asklepios investigators. Noninvasive (Input) Impedance, Pulse Wave Velocity, and Wave Reflection in Healthy Middle-Aged Men and Women. *Hypertension*. 2007;49:1248–1255.
9. Burattini R. Downstream from the Heart Left Ventricle. In: *Modelling Methodology for Physiology and Medicine*. Elsevier; 2014:503–525.
10. Burattini R, Knowlen GG, Campbell KB. Two arterial effective reflecting sites may appear as one to the heart. *Circulation Research*. 1991;68:85–99.
11. Li JK, Melbin J, Noordergraaf A. Directional disparity of pulse reflection in the dog. *The American Journal of Physiology*. 1984;247:H95–99.
12. Milnor WR. *Hemodynamics*. 2nd ed. Baltimore: Williams & Wilkins; 1989.
13. Milnor WR, Bertram CD. The relation between arterial viscoelasticity and wave propagation in the canine femoral artery in vivo. *Circulation Research*. 1978;43:870–879.
14. Mitchell GF, Parise H, Benjamin EJ, Larson MG, Keyes MJ, Vita JA, Vasan RS, Levy D. Changes in Arterial Stiffness and Wave Reflection With Advancing Age in Healthy Men and Women: The Framingham Heart Study. *Hypertension*. 2004;43:1239–1245.
15. Mitchell GF, Wang N, Palmisano JN, Larson MG, Hamburg NM, Vita JA, Levy D, Benjamin EJ, Vasan RS. Hemodynamic Correlates of Blood Pressure Across the Adult Age Spectrum: Noninvasive Evaluation in the Framingham Heart Study. *Circulation*. 2010;122:1379–1386.
16. Torjesen AA, Wang N, Larson MG, Hamburg NM, Vita JA, Levy D, Benjamin EJ, Vasan RS, Mitchell GF. Forward and Backward Wave Morphology and Central Pressure Augmentation in Men and Women in the Framingham Heart Study. *Hypertension*. 2014;64:259–265.
17. Izzo JL. Brachial vs. Central Systolic Pressure and Pulse Wave Transmission Indicators: A Critical Analysis. *American Journal of Hypertension*. 2014;27:1433–1442.

18. Burattini R, Gnudi G. Computer identification of models for the arterial tree input impedance: Comparison between two new simple models and first experimental results. *Medical & Biological Engineering & Computing*. 1982;20:134–144.
19. Burattini R, Campbell KB. Modified asymmetric T-tube model to infer arterial wave reflection at the aortic root. *IEEE Transactions on Biomedical Engineering*. 1989;36:805–814.
20. Shroff SG, Berger DS, Korcarz C, Lang RM, Marcus RH, Miller DE. Physiological relevance of T-tube model parameters with emphasis on arterial compliances. *The American Journal of Physiology*. 1995;269:H365–374.
21. Dujardin J-PL, Stone DN. Characteristic impedance of the proximal aorta determined in the time and frequency domain: a comparison. *Medical & Biological Engineering & Computing*. 1981;19:565–568.
22. Lucas CL, Wilcox BR, Ha B, Henry GW. Comparison of time domain algorithms for estimating aortic characteristic impedance in humans. *IEEE Transactions on Biomedical Engineering*. 1988;35:62–68.
23. Li JK-J. *The arterial circulation physical principles and clinical applications*. Totowa, N.J.: Humana Press; 2000.
24. Mitchell GF, Tardif J-C, Arnold JMO, Marchiori G, O'Brien TX, Dunlap ME, Pfeffer MA. Pulsatile Hemodynamics in Congestive Heart Failure. *Hypertension*. 2001;38:1433–1439.
25. Chirinos JA, Segers P. Noninvasive Evaluation of Left Ventricular Afterload: Part 2: Arterial Pressure-Flow and Pressure-Volume Relations in Humans. *Hypertension*. 2010;56:563–570.
26. Swillens A, Taelman L, Degroote J, Vierendeels J, Segers P. Comparison of Non-Invasive Methods for Measurement of Local Pulse Wave Velocity Using FSI-Simulations and In Vivo Data. *Annals of Biomedical Engineering*. 2013;41:1567–1578.
27. Segers P, Swillens A, Taelman L, Vierendeels J. Wave reflection leads to over- and underestimation of local wave speed by the PU- and QA-loop methods: theoretical basis and solution to the problem. *Physiological Measurement*. 2014;35:847–861.
28. Shroff SG, Janicki JS, Weber KT. Evidence and quantitation of left ventricular systolic resistance. *The American Journal of Physiology*. 1985;249:H358–370.
29. Reymond P, Merenda F, Perren F, Rufenacht D, Stergiopulos N. Validation of a one-dimensional model of the systemic arterial tree. *AJP: Heart and Circulatory Physiology*. 2009;297:H208–H222.
30. Westerhof N, Stergiopulos N, Noble MIM. *Snapshots of hemodynamics an aid for clinical research and graduate education*. New York: Springer; 2010.